Exit Flow Measurements of a Centrifugal Pump Impeller

Soon-Sam Hong, Shin-Hyoung Kang*

School of Mechanical and Aerospace Engineering, Seoul National University,
Seoul 151-742, Korea

Discharge flows from a centrifugal pump impeller with a specific speed of 150 [rpm, m³/min, m] were experimentally investigated. A large axisymmetric collector instead of a volute casing was installed to obtain circumferentially uniform flow, i.e. without interaction of the impeller and the volute. The unsteady flow was measured at the impeller exit and vaneless diffuser using a hot film probe and a pressure transducer. The flow at impeller exit showed pronounced jet-wake flow patterns. The wake, which was on the suction/hub side at high flow rate, became enlarged pitchwisely on both the hub and the shroud side as the flow rate decreases. The pitchwise non-uniformity of the flow rapidly decreased along the downstream and the non-uniformity almost disappeared at radius ratio of 1.18 for medium flow rate. The mean vaneless diffuser flow was reasonably predicted using a one dimensional analysis when an empirical constant was used to specify the skin friction coefficient. The data can be used for a centrifugal pump impeller design and validation of CFD codes and flow modeling.

Key Words : Centrifugal Pump, Impeller Discharge Flow, Jet-Wake, Vaneless Diffuser, Hot-Film Probe

Nomenclature

b	: Passage width
C	: Absolute velocity
C_{slip}	: Slip velocity
PS	: Pressure side
Q	: Flow rate
r	: Radius
Re	: Reynolds number
S	: Suction side to pressure side coordinate
SHR	: Shroud
SS	: Suction side
U	: Peripheral velocity of impeller
W	: Relative velocity
z	: Hub to shroud coordinate
α	: Absolute flow angle from tangential direction
β	: Relative flow angle from tangential direction
ϕ	: Flow coefficient, C_{m2}/U_2
ν	: Kinematic viscosity
ρ	: Density
σ	: Slip factor, $1 - C_{slip}/U_2$
ψ	: Total pressure coefficient normalized by $0.5\rho U_2^2$
ψ_s	: Static pressure coefficient normalized by $0.5\rho U_2^2$

Subscripts

2	: Impeller exit
m	: Radial component
t	: Tangential component

* Corresponding Author,
 E-mail : kangsh@snu.ac.kr
 TEL : +82-2-880-7113; **FAX** : +82-2-883-0179
 Professor, School of Mechanical and Aerospace Engineering, Seoul National University, Seoul 151-742, Korea. (Manuscript **Received** July 30, 2001; **Revised** June 17, 2002)

1. Introduction

A centrifugal impeller is usually followed by downstream diffuser or volute. Matching of discharge flow from the impeller to the downstream components is quite important for good performance of a pump. The discharge flow is

unsteady and highly three dimensional due to interaction between the components. Even without interaction, there are still needs of investigation of the discharge flow from the impeller. The measured data will be used for validation of various CFD codes and flow modeling.

Many investigations have been concerned with centrifugal compressors. Eckardt (1975) measured jet-wake discharge flow from an impeller. Johnson and Moore (1983) measured the flow in the impeller, and showed how the wake's size decreased as the flow rate increased. Inoue and Cumpsty (1984) measured the detailed flow in vaneless and vaned diffusers. Pinarbasi and Johnson (1994) measured three dimensional velocity field within a vaneless diffuser at off design flow condition. Choi (1994a, 1994b) performed aerodynamic and acoustic measurements on a centrifugal water pump using air as a working fluid and related this flow field to noise generation in an impeller.

For centrifugal pumps, Murakami et al. (1980) measured flow patterns in the centrifugal pump impellers using a rotating yaw probe and an oil surface flow method. Hamkins and Flack (1987) measured velocities within an impeller and volute using a laser velocimeter and indicated that flow slip was 30 percent higher for the unshrouded impeller than for the shrouded impeller. Asakura et al. (1999) measured the discharge flow in cavitating condition and found that flow slip and hydraulic loss increased when the cavitation occurred.

Most of the works for pumps were obtained from the impellers followed by non-axisymmetric volute casings, so the discharge flow might not be uniform along the volute circumference. The present study aims to investigate the discharge flow field and to obtain a data base without any interaction between the impeller and the downstream components. Instead of a volute, an axisymmetric collecting chamber was installed, so the discharge flow was circumferentially uniform except for blade-to-blade unsteadiness. Unsteady velocity measurements at the impeller exit and in the vaneless diffuser were done using a hot film probe and a pressure transducer.

2. Experimental Facility and Instrumentation

2.1 Test rig and impeller

An outline of the test rig is shown in Fig. 1. The impeller is driven by a variable speed motor in a closed-loop facility. The flow rate is measured by a flow nozzle and controlled by a regulating valve. The test section is composed of an impeller, a vaneless diffuser, and a collector. The shrouded centrifugal impeller, shown in Fig. 2, has a tip diameter of 260 mm and six blades of 25 deg outlet angle from tangential direction. The impeller has a low specific speed
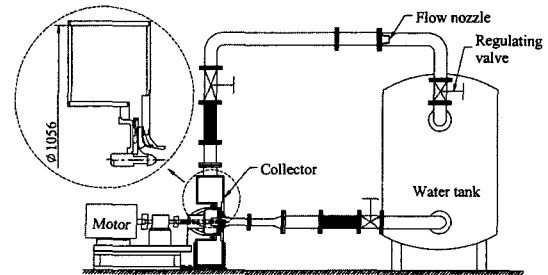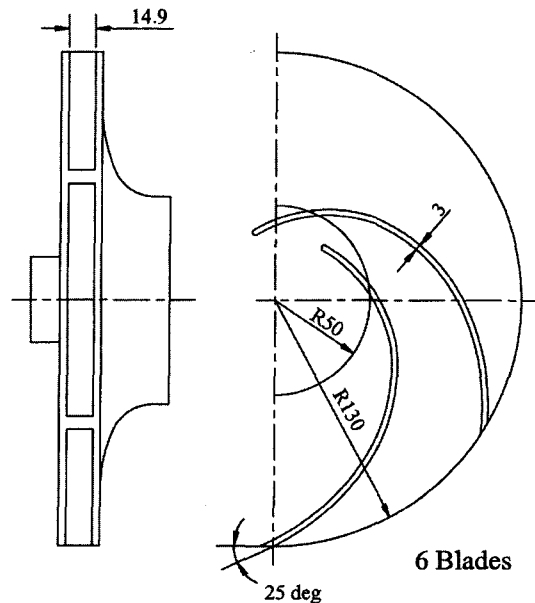

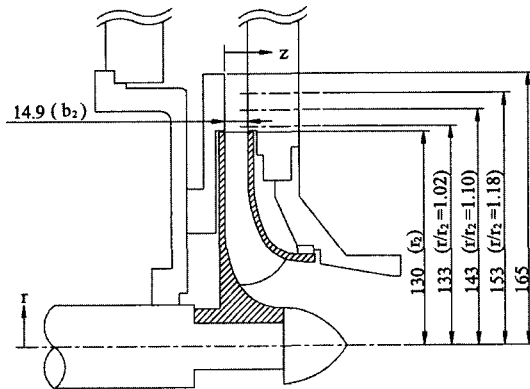Fig. 1 Schematic view of the test rig

Fig. 2 Impeller geometry

Fig. 3 Cross section of the impeller and diffuser and the locations of measurements; $r/r_2=1.02$, 1.10 and 1.18

of 150 [rpm, m³/min, m]. The rotational speed is controlled by an inverter and fixed at 300 rpm for the present experiments. The vaneless diffuser has parallel walls of 14.9 mm width and 330 mm outlet diameter. The diffuser is followed by a collector, which has a cross section of 300 mm by 300 mm. The axisymmetric collector was designed to provide circumferentially uniform flow condition at the impeller discharge. The schematic, meridional view of the centrifugal pump impeller shown in Fig. 3 illustrates also the locations of measurement. The velocity and pressure are measured at three radial locations downstream of the impeller $(r/r_2=1.02, 1.10, 1.18)$. Velocities are measured at 8 points from the hub to shroud $(z=1, 2, 4, 6, 8, 10, 12,$ and 14 mm$)$.

2.2 Instrumentation

A single hot film probe of I-type (Dantec 55R11 fiber-film probe) is used to measure the instantaneous velocities and flow directions. Two velocity components in the radial and circumferential direction are measured because the axial component is considered to be very small. Measurements are taken at two probe orientations 60 deg apart. This method is similar to the single hot wire probe method used by Inoue and Cumpsty (1984). A pressure transducer (Kulite XTM-190) is used for wall static pressure measurements on the shroud side diffuser wall. The total pressure is calculated from the measured

static pressure and the velocity.

The sampling rate of the A–D converter is 3 kHz, so that 100 data are taken over one blade pitch at 300 rpm. Since the discharge flow is highly turbulent, a phase-locked sampling and ensemble averaging technique is used. From a photo sensor one pulse is produced per shaft revolution and used as a trigger signal for ensemble average. Unsteady signal from the hot film probe or a pressure transducer is acquired together with the trigger signal and then data reduction is carried out by a ensemble averaging technique.

3. Results and Discussion

3.1 Instantaneous flow field

In Fig. 4 static pressure at impeller exit is plotted against flow rate. The original pump with the impeller and the volute shows the best efficiency at $\phi=0.069$. The flows are measured for three flow rates, i.e. $\phi=0.049$, 0.069 and 0.084. The averaged flow rate, which is calculated by integrating the measured radial velocity at the impeller exit, is compared with the values obtained from the flow meter. At design and high flow rate the two measurements coincide with each other with an error smaller than 4 percent. However, at low flow rate condition the integrated flow rate is higher than the flow meter reading by approximately 15 percent. Since the absolute flow angle at the low flow rate is about 5 deg from the tangential direction, an angle shift of 0.5 deg can make about 10 percent error in the integrated flow rate.

Figure 5 shows the ensemble averaged velocity components at the mid passage width of the impeller exit for the flow rate of $\phi=0.069$. Typical jet-wake flow pattern is observed in the figure, where the velocity components are shown over two blade pitches. Radial velocity on the pressure side is higher than that on the suction side. Relative velocity is also higher on the pressure side, although the tangential velocity shows an opposite trend to the relative velocity. The small value of radial velocity relative to the tangential one results in small flow angle.
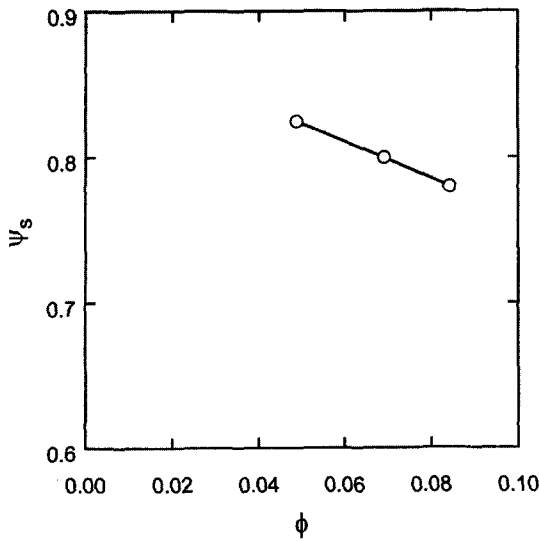
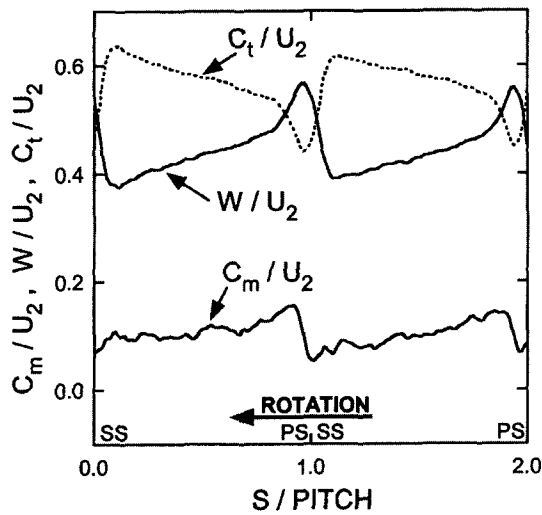Fig. 4 Measured performance map of the pump

Fig. 5 Variation of ensemble averaged velocities; $z/b_2=0.54$, $r/r_2=1.02$, $\phi=0.069$

(a) $\phi=0.084$

(b) $\phi=0.069$

(c) $\phi=0.049$

Fig. 6 Contours of radial velocity (C_m/U_2) at three flow rates; $r/r_2=1.02$

The extent and location of the wake are affected by the flow rate and impeller geometry. In order to observe jet-wake flow pattern, conventional contours of radial velocity at three flow rates are illustrated in Fig. 6. The actual ratio of one blade pitch to impeller exit width (b_2) is 9.1, although in Fig. 6 the physical scale of the frame is modified such that the spanwise scale is about 5 times the pitchwise one. Velocity distributions over one blade pitch are shown in this figure,
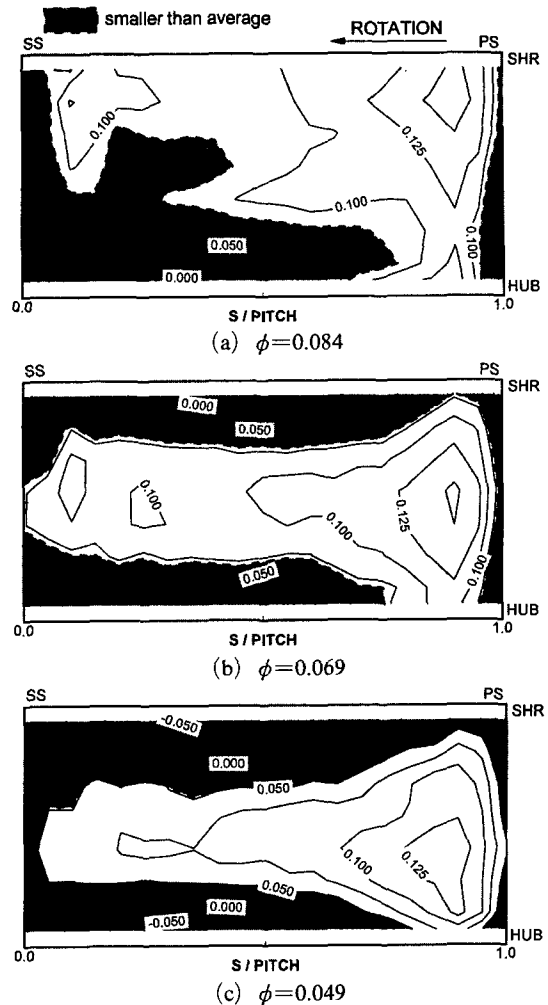
where the velocity levels smaller than the mean values are shaded to show the low radial velocity wake region. The wake region is located near suction/hub side at $\phi=0.084$. When the flow rate is reduced to $\phi=0.069$, the wake exist on the shroud side as well as the hub side. Further decrease of the flow rate to $\phi=0.049$ causes the wake to be enlarged on the shroud side. Eckardt (1976), Johnson and Moore (1983), and Inoue and Cumpsty (1984) also showed that the wake altered its area and location with flow rate.

Figure 7 shows the ensemble averaged flow at three radii for $\phi=0.069$. In pitchwise direction, 20 data of measured 100 data per pitch are shown.
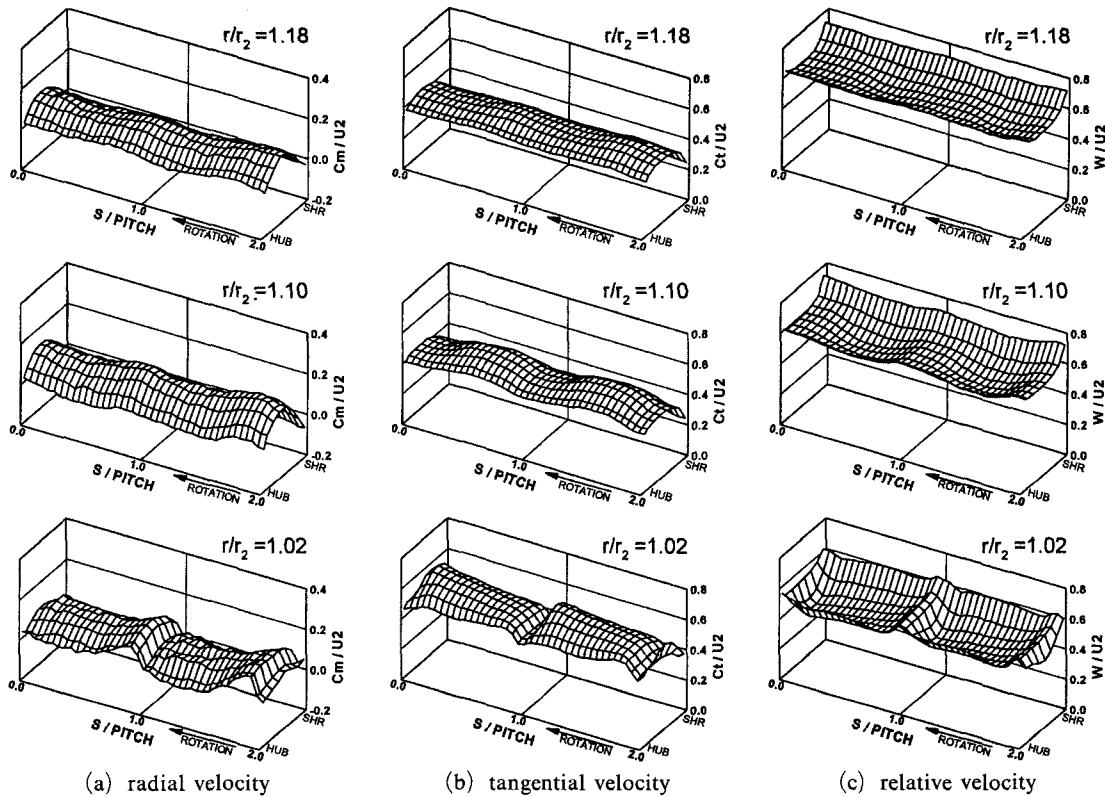
(a) radial velocity   (b) tangential velocity   (c) relative velocity

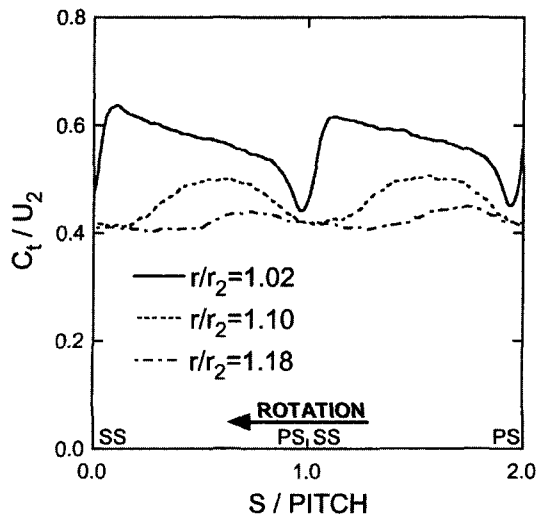**Fig. 7** Distributions of ensemble averaged flow at three radii ; $\phi=0.069$

Fig. 8 Variation of tangential velocity with radius ; $z/b_2=0.54$, $\phi=0.069$

As the radius increases, the pitchwise non-uniformity of the flow becomes smaller due to mixing between the jet and wake. The jet and wake mix out rapidly to the radial direction, and non-uniformity almost disappears at $r/r_2=1.18$. Tangential velocities measured at the mid width $(z/b_2=0.54)$ are shown in Fig. 8, where the radial variation of pitchwise non-uniformity is clearly observed.

3.2 Mean flow field

The ensemble averaged flow is pitchwise-averaged again to see the spanwise variation of mean flow. Figure 9 shows the mean flow measured at three flow rates. The radial velocity showing a nearly linear spanwise distribution at $\phi=0.084$, becomes a symmetric boundary layer type at $\phi=0.049$. Reverse flow is observed on both shroud and hub at $\phi=0.049$. The radial velocity variation with the flow rate is larger on the shroud side than the hub side. The tangential velocity increases on the whole as the flow rate decreases. The absolute flow angle decreases with the flow rate and has very similar pattern to the
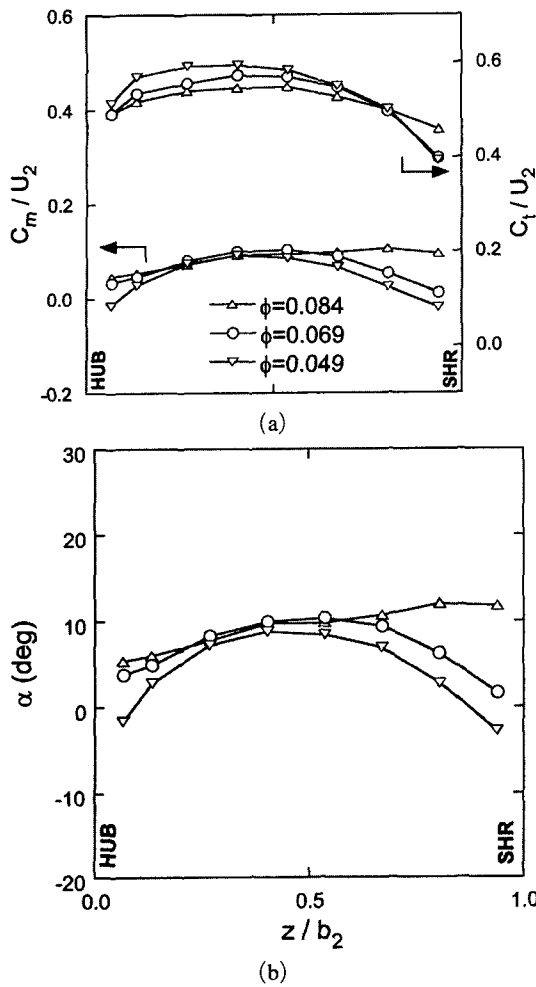
Fig. 9 Hub to shroud mean (a) velocities and (b) absolute flow angle variation at three flow rates ; $r/r_2=1.02$

radial velocity.

It should be noted here that the discharge flow is circumferentially uniform because the impeller is followed by an axisymmetric collector. The averaged results can provide data for design and performance prediction of impeller, diffuser, and volute. To see general view of flow change with the flow rate, the pitchwise-averaged flow is span-wise-averaged again and the results are shown in Fig. 10. Tangential velocity increases as the flow rate decreases. Absolute and relative flow angle decrease with the flow rate. The relative flow angle is higher than the absolute flow angle, and the difference between the two angles increases
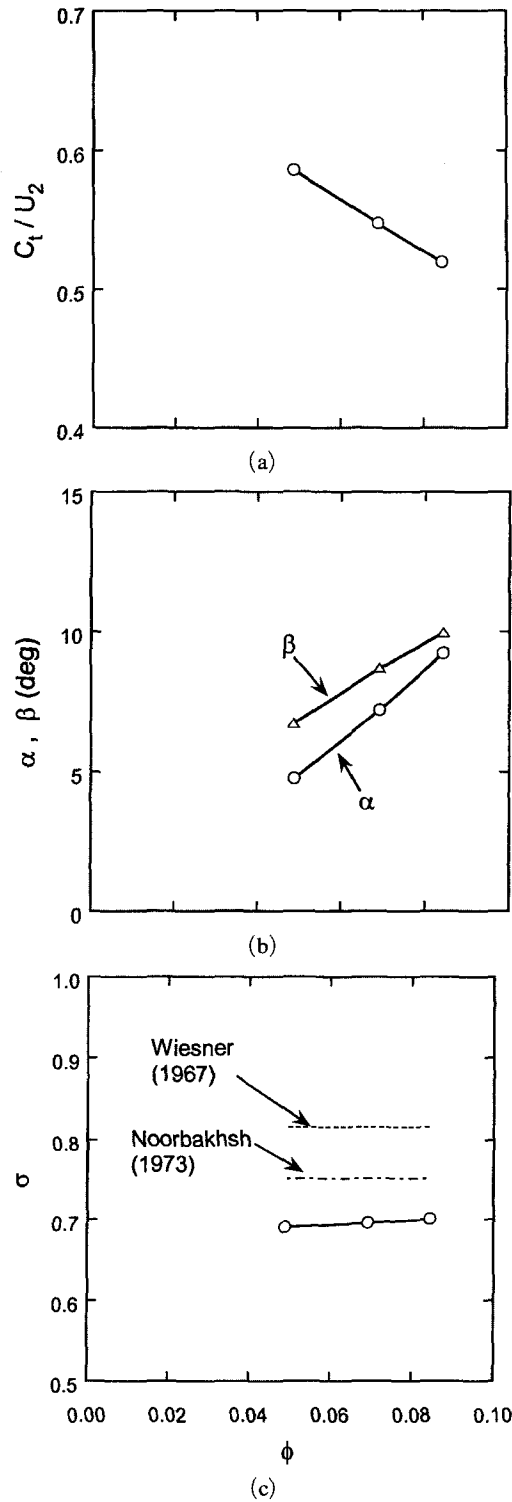

Fig. 10 Variation of averaged (a) tangential velo city (b) flow angles and (c) slip factor $r/r_2=1.02$

with decrease in the flow rate. Slip factor shows an almost constant value of 0.7 for measured flow rate. Predicted value of slip factor for the present impeller is 0.82 from the correlation of Wiesner (1967) and 0.75 from Noorbakhsh (1973). The former correlation has often been found useful for the compressor impellers and the latter is based on the test results of several pump impellers. Slip factors from both correlations are function of only blade number and exit blade angle, regardless of specific speed. The specific speed of the present test impeller is lower than that of Noorbakhsh (1973), that is, the ratio of

Fig. 11 Hub to shroud mean (a) velocities and (b) absolute flow angle variation at three radii ; $\phi=0.069$

exit width to radius (b_2/r_2) of the present impeller is three times smaller. That is probably the reason for the lower slip factor of present test impeller than the empirical correlation of Noorbakhsh (1973).

Figure 11 shows the variation of mean flow with radius for the flow rate of $\phi=0.069$. Radial velocity shows gradual variation with radius. The value of tangential velocity decreases with increase in radius due to angular momentum conservation and wall skin friction. The absolute flow angle remains almost constant at about 7.5 deg, but the angle difference between the mid passage and side walls generally increases with radius. This is attributed to the fact that the flow angle near walls decreases with radius due to wall skin friction.

Spanwise-averaged flow along the vaneless diffuser permits comparison between the measured data and the one dimensional vaneless diffuser performance model of Stanitz (1952). Model equations in the appendix can be solved directly by a numerical integration technique between the impeller exit and the outer radius of the vaneless diffuser space. But, it is important to specify a proper value of skin friction coefficient in order to get reasonable predictions. Japikse (1982) used the following form of skin friction coefficient :

$$C_f = k(1.8 \times 10^5/Re)^{0.2} \qquad (1)$$

where Re is the Reynolds number defined as $Re=2Cb/\nu$. Japikse et al. (1997) indicated that an empirical value of $k=0.01$ was frequently used based on a review of different vaneless diffusers in industrial machines, however, applications have existed where a value one-half this level or nearly twice this level has been necessary. The predicted results for the present test for various k are shown in Fig. 12 with k varied. The calculations begin at the impeller exit, where the initial values are given, and proceed through the vaneless diffuser. According to the results, $k=0.01$ is reasonable for the present test. The flow varies abruptly close to the impeller exit and this seems to be why the prediction shows a little difference from the measurement at $r/r_2=1.10$.
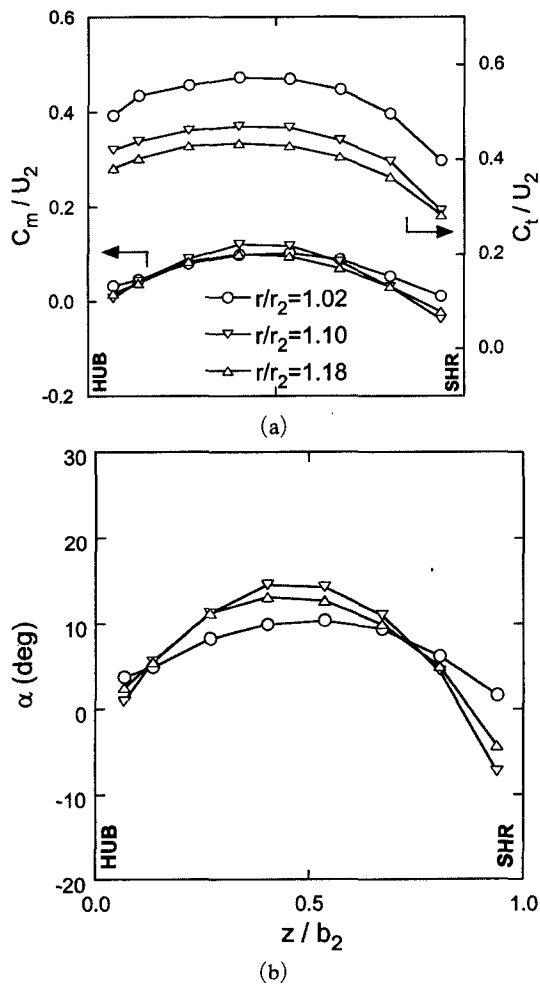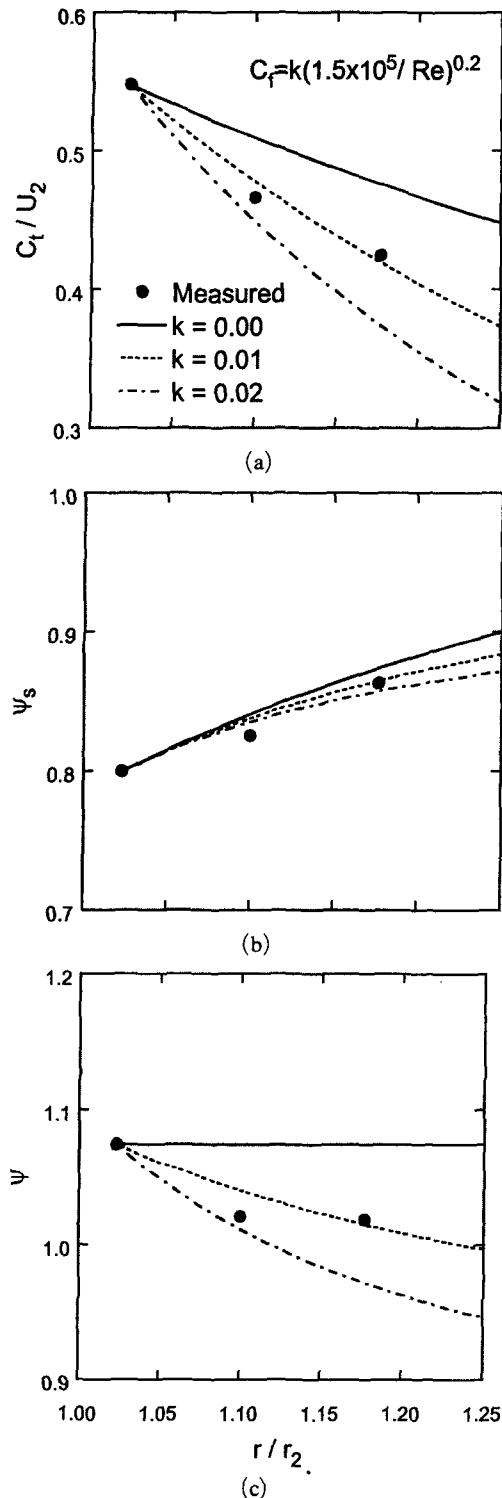
Fig. 12 Calculated (a) tangential velocity (b) static pressure and (c) total pressure coefficient distribution in vaneless diffuser ; ϕ=0.069

4. Conclusions

The instantaneous velocity measured at the exit of a centrifugal pump impeller shows that the location and area of wake changes with the flow rate. The wake region is located on suction/hub side for high flow rate, however both on the shroud and hub side for the low and design flow rate. Pitchwise non-uniformity of the flow decreases due to mixing between jet and wake at the downstream, and the non-uniformity almost disappears at r/r_2=1.18 for ϕ=0.069.

A change in radial velocity and slip factor with flow rate on the shroud side is larger than that on the hub side. Spanwise-averaged tangential velocity decreases with flow rate, which results in the decrease in absolute and relative flow angle with flow rate. Slip factor shows a constant value of 0.7 for measured flow rates. With an increase in measuring radius, radial and tangential velocity decrease and absolute flow angle shows a constant value of 7.5 deg.

Acknowledgment

References

Asakura, E., Hasegawa, Y., Kikuyama, K. and Nomura, R., 1999, "Study on Exit Flow of a Centrifugal Pump Impeller in Cavitating Condition," *Proceedings of the 3rd ASME/JSME Joint Fluids Engineering Conference*, FEDSM99-7211.

Choi, J. S., 1994a, "Discharge Flow Measurements of a Centrifugal Turbomachinery," *KSME International Journal*, Vol. 8, pp. 152~160.

Choi, J. S., 1994b, "Aerodynamic Noise Generation in Centrifugal Turbomachinery," *KSME International Journal*, Vol. 8, pp. 161~174.

Eckardt, D., 1975, "Instantaneous Measurements in the Jet-Wake Discharge Flow of a Centrifugal Compressor Impeller," *ASME Journal of Engineering for Power*, pp. 337~346.

Eckardt, D., 1976, "Detailed Flow Investigations within a High Speed Centrifugal Compressor Impeller," *ASME Journal of Fluids Engineering*, pp. 390~402.

Hamkins, C. P. and Flack, R. D., 1987, "Laser Velocimeter Measurements in Shrouded and Unshrouded Radial Flow Pump Impellers," *ASME Journal of Turbomachinery*, Vol. 109, pp. 70~76.

Inoue, M. and Cumpsty, N. A., 1984, "Experimental Study of Centrifugal Impeller Discharge Flow in Vaneless and Vaned Diffusers," *ASME Journal of Engineering for Gas Turbine and Power*, Vol. 106, pp. 455~467.

Japikse, D., 1982, "Advanced Diffuser Levels in Turbocharger Compressors and Component Matching," *Turbocharging and Turbochargers*, IMechE, C45/82, pp. 143~155.

Japikse, D., Marscher, W. D. and Furst, R. B., 1997, *Centrifugal Pump Design and Performance*, Concepts ETI, Inc., pp. 3-10~3-11.

Johnson, M. W. and Moore, J., 1983, "The Influence of Flow Rate on the Wake in a Centrifugal Impeller," *ASME Journal of Engineering for Power*, Vol. 105, pp. 33~39.

Murakami, M., Kikuyama, K. and Asakura, E., 1980, "Velocity and Pressure Distributions in the Impeller Passages of Centrifugal Pumps," *ASME Journal of Fluids Engineering*, Vol. 102, pp. 420~426.

Noorbakhsh, A., 1973, "Theoretical and Real Slip Factor in Centrifugal Pumps," von Karman Institute for Fluid Dynamics, Technical Note 93.

Pinarbasi, A. and Johnson, M. W., 1994, "Off Design Flow Measurements in a Centrifugal Compressor Vaneless Diffuser," *ASME Paper 94-GT-42*.

Stanitz, J. D., 1952, "One-Dimensional Compressible Flow in Vaneless Diffusers of Radial and Mixed-Flow Centrifugal Compressors, Including Effects of Friction, Heat Transfer and Area Change," NACA Technical Note 2610.

Wiesner, F. J., 1967, "A Review of Slip Factors for Centrifugal Impellers," *ASME Journal of Engineering for Power*, Vol. 89, pp. 558~572.

Appendix

Stanitz (1952) developed an analysis method for one-dimensional, compressible flow with friction, heat transfer, and area change in vaneless diffusers with arbitrary profiles in the axial-radial plane. When the method is applied to present one-dimensional, incompressible flow with friction in parallel-walled vaneless diffuser with radial plane, the following equations are obtained:

$$C_m \frac{dC_m}{dr} - \frac{C_t^2}{r} + C_f \frac{C^2 \sin \alpha}{b} + \frac{1}{\rho} \frac{dP}{dr} = 0 \quad (2)$$

$$C_m \frac{dC_t}{dr} + \frac{C_m C_t}{r} + C_f \frac{C^2 \cos \alpha}{b} = 0 \quad (3)$$

$$\frac{1}{C_m} \frac{dC_m}{dr} + \frac{1}{r} = 0 \quad (4)$$

Eqs. (2)~(4) represent the radial equilibrium, tangential equilibrium and continuity respectively.